Available online at www.sciencedirect.com

ScienceDirect

Advances in Space Research 61 (2018) 552–566

ADVANCES IN SPACE RESEARCH (a COSPAR publication)

www.elsevier.com/locate/asr

Radio sounding of the solar wind acceleration region with spacecraft signals

Oleg I. Yakovlev [a], Yuri V. Pisanko [b,*]

[a] Institute of Radio Engineering and Electronics of Russian Academy of Sciences, Vvedenskogo sq. 1, Fryazino, Moscow Region 141190, Russia
[b] Institute of Applied Geophysics, Rostokinskaya st. 9, Moscow 129128, Russia

Received 5 April 2017; received in revised form 14 August 2017; accepted 30 October 2017
Available online 8 November 2017

Abstract

Data from coronal radio-sounding experiments carried out on various interplanetary spacecraft are used to derive the empirical radial dependence of solar wind velocity and density at heliocentric distances from 3 to 60 solar radii for heliolatitudes below 60° and for low solar activity. The radial dependencies of solar wind power and acceleration are derived from these results. Summaries of the radial behavior of characteristic parameters of the solar wind turbulence (e.g., the spectral index and the inner and outer turbulence scales), as well as the fractional density fluctuation, are also presented. These radio-sounding results provide a benchmark for models of the solar wind in its acceleration region.

Keywords: Solar wind; Velocity; Density; Power; Turbulence; Plasma

1. Introduction

Spacecraft launched to planets and deep space radio-communication ground stations gave the opportunity to carry out unique experiments on radio sounding the solar plasma environment (Goldstein, 1969; Yakovlev et al., 1974). In such experiments deep space radio-communication ground stations were used as complex radio-physical installations with large parabolic antennas, high sensitive receivers, frequency standards, precise timing, signal filtering, measuring and registering. The facilities allowed obtaining detailed information on the propagation of decimeter and centimeter radio waves in space and determining plasma parameters in the solar wind acceleration region on this basis. The Russian system of deep space radio communication used two wavelengths $\lambda_1 = 32$ cm and $\lambda_2 = 5.07$ cm, the US one – three wavelengths $\lambda_3 = 13$ cm, $\lambda_4 = 3.6$ cm, $\lambda_5 = 0.96$ cm. Radio-sounding experiments were carried out using monochromatic spacecraft signals of high frequency stability during radio transmission sessions to the Earth lasting from a few minutes to many hours. Every experiment lasted 2–3 months, when the ray path approached the Sun and then moved away from the Sun. Based on these radio propagation data one may determine coronal plasma parameters at heliocentric distances from 3 to 60 solar radii.

To study solar plasma environment characteristics one uses the experimental data on radio delay and radio fluctuations as well as the theory of radio wave propagation in inhomogeneous medium. Exploiting the complex experimental technique along with the statistics of signal processing and the theory of radio wave propagation one derives the information on velocity, electron concentration and turbulence of medium in the solar wind acceleration region.

* Corresponding author.
E-mail addresses: oiy117@ire216.msk.su (O.I. Yakovlev), pisanko@ipg.geospace.ru (Y.V. Pisanko).

https://doi.org/10.1016/j.asr.2017.10.052
0273-1177/

This paper presents an overview of the heliocentric distance dependence of solar plasma environment parameters as derived from radio sounding using spacecraft signals. The heliocentric distance, denoted r in the following, is expressed in solar radii units. The described solar plasma environment parameters are related to heliolatitudes below 60° for relatively low and moderate solar activity.

2. Solar wind velocity

There are several means to measure the solar wind velocity via radio sounding. These are based on the analysis of radio signals received at one or two widely spaced ground stations.

The first, elaborated in Efimov et al. (1981), Yakovlev et al. (1980a, 1989), exploits the peculiarities of frequency fluctuations registered at two ground stations spaced on the large distance BB_1. In Fig. 1 one can see: the solar center – O, two spaced ground stations (B and B_1), a spacecraft – A, two ray paths AB and AB_1. In the region of the closest approach to the Sun defined by impact parameters $OC = r_0$ and $OC_1 = r_1$ the points C and C_1 are spaced on the distance $\Delta r = r_1 - r_0$, therefore the distance Δr is mainly determined by the distance BB_1 between ground stations. Radial moving solar wind plasma inhomogeneities pass through C and C_1 areas at different time moments, so that similar fluctuations of frequency will be consecutively observed at the ground stations. These appear at the station B_1 first and at the station B next, so that synchronous observations of frequency fluctuations

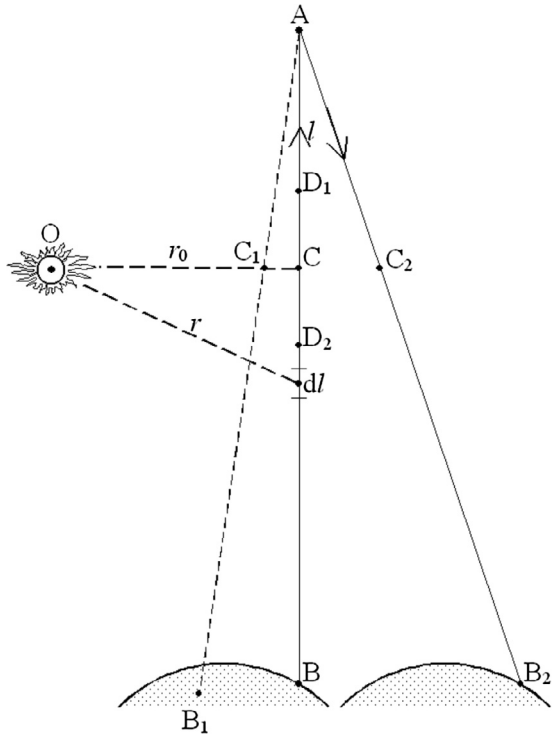

Fig. 1. Coronal sounding experiments under spaced radio reception.

will demonstrate the time delay Δt. One calculates the cross-correlation function B_f of frequency fluctuations registered at two ground stations B and B_1 and determines the time delay Δt corresponding to the maximum of the function B_f. The solar wind velocity is equal to $V = \Delta r/\Delta t$. One can precisely calculate the time delay Δt only when the function B_f has the sufficiently narrow maximum which is the case of "frozen in" plasma inhomogeneities carried by the solar wind unchangeably through the area C_1 first and the area C next. Experiments revealed that the method gave satisfactory results when the maximum of cross-correlation function was greater than 0.6 and the stations B and B_1 were spaced on several thousand kilometers. The idea and the geometry of the method imply that the measured velocity corresponds to the movement of plasma inhomogeneities of several thousand kilometers in scale. It is necessary to bear in mind that radio fluctuations could be caused by plasma inhomogeneities of various origin moving with various velocities. Such a situation could be realized in case of both evident waves of plasma density and two almost regular solar wind streams or several plasma ejections (Efimov et al., 2003,2005b). To determine "true" bulk solar wind velocity V(r) it is important to analyze in detail the experimental correlation function of radio frequency fluctuations $B_f(\tau)$ obtained in the specified communication session for known value of the heliocentric distance r. The presence of single narrow maximum of $B_f(\tau)$, whose value is greater than 0.6, testifies to single well determined solar wind velocity. If diffused correlation function $B_f(\tau)$, whose value is lower than 0.6, is registered in a communication session, then the data obtained in this communication session are eliminated as doubtful. From time to time (but rarely) $B_f(\tau)$ with two well defined maxima was registered, and this indicated the two-stream plasma structures.

The second is based on the features of the operation of the space communication system in the coherent response regime when the spacecraft situated at the point A receives the signal from the ground transmitter situated at the point B and re-transmits the signal to the ground receiver situated at the same point B (Yakubov et al., 1991). Due to the Earth orbital motion the ground receiver appears at the point B_2 after the time $\Delta t = 2ABc^{-1}$ (c - is the speed of light). In the coherent mode radio waves propagate along the ray path BA first and the ray path AB_2 next, so that appear will frequency fluctuations of radio waves passing through the area C first and the area C_2 next. In such regime the auto-correlation function of frequency fluctuations registered by the ground receiver has the maximum at the time Δt connected to the solar wind velocity V via the expression $V = CC_2/\Delta t$. The distance CC_2 is determined by the geometry and the Earth orbital motion speed. It is supposed that the measured solar wind velocity reflects the motion of plasma inhomogeneities of the CC_2 scale. This method of measuring the solar wind velocity requires an uplink and a downlink. The time delay depends not only on the velocity of the solar wind, but also on the position of

the main contribution along the radio ray path in the corona (Paetzold et al., 2012). Under quasi-stationary conditions we assume that the main contribution to the frequency fluctuations occurs at the proximate point to the Sun along the ray path. However, examples have been reported (probably under non-stationary conditions) where this is definitely not true (Paetzold et al., 2012).

The third, pioneering by radio astronomers, is based on the relationship between the velocity of transportation of inhomogeneous medium through the radio link and the peculiarity of the temporal spectrum of radio amplitude fluctuations recorded at a single ground station. In the theory of radio wave propagation in statistically inhomogeneous medium (Ishimaru, 1978; Yakovlev, 2002) it is shown that one can determine the frequency of fluctuations F_0 as the function of velocity V of the medium as follows:

$$V = F_0\left(\frac{2\pi l_1 l_2 \lambda}{l_1 + l_2}\right)^{1/2} \quad (1)$$

if amplitude fluctuations are small. The use of amplitude fluctuations to measure the velocity implies that one measures the velocity of plasma inhomogeneities of the first Fresnel zone scale that is several hundred kilometers.

Because three methods described above encountered a difficulty for $r \leq 7$, the fourth meant for small heliocentric distances was elaborated. This is based on the change of the spectral line bandwidth (or the intensity of frequency fluctuations) when the ray path approaches to or moves away from the Sun (Efimov et al., 1977, 2017). According to Efimov et al. (1977) the dispersion of radio frequency fluctuations σ_f^2 (or spectral line width square Δf^2) depends on the velocity of plasma inhomogeneity motion through the radio link V_1 as follows:

$$\sigma_f^2 \propto V_1^{p-2} \quad (2)$$

where p is the spectral index of plasma turbulence spatial spectrum. The velocity V_1 in Eq. (2) is equal to the sum of (or difference between) the solar wind velocity V and the velocity dr_0/dt of the ray path approach (or move away) due to the motions of the Earth and a spacecraft. Therefore

$$\sigma_f \propto (V \pm dr_0/dt)^{\frac{p-2}{2}} \quad (3)$$

where the sign "+" corresponds to the ray path approach to the Sun, and the sign "−" corresponds to the motion of the ray path away from the Sun. Eq. (3) allows the determination of the solar wind velocity if V and dr_0/dt are of the same scale and σ_f is given both for the ray path approach to the Sun and for the ray path motion away from the Sun. From experimental heliocentric distance dependencies $\sigma_f(r)$ obtained in both cases one can calculate the ratio $\beta = \sigma_{ap}/\sigma_{ma}$. In case of $p = 3$ for $r \leq 7$ Eq. (3) is degenerated into the equation:

$$V = \left(\frac{\beta^2 + 1}{\beta^2 - 1}\right)\frac{dr_0}{dt} \quad (4)$$

Eq. (4) gives the solar wind velocity under known (from the spacecraft trajectory data) dr_0/dt and measured values of β. As is easy to see the method has some uncertainty: during the stage of ray path approach to the Sun and the stage of ray path motion away from the Sun (which are spaced in time when the spacecraft moves along the trajectory) r_0 can (in some moments) be of the same value and according to Eq. (4) so does the solar wind velocity. Therefore Eq. (4) estimates the solar wind velocity only in case of quiet inactive Sun when it does not vary strongly during a month.

Several attempts to derive the solar wind velocity heliocentric distance dependence were undertaken in 1976–1977. The results are shown in Figs. 2 and 3 where the dependencies derived by different methods are marked by different signs. The results of the first method are marked by squares, the second – by triangles, the third – by circles, the fourth – by crosses. The reliable velocity heliocentric distance dependence in the solar wind acceleration region was obtained from radio signals of the "Venera-10" spacecraft (Efimov et al., 1977, 1981; Kolosov et al., 1982; Yakovlev et al., 1980a). The dependence is shown in the upper graph of Fig. 2. The measurements were carried out at the wavelength λ_1 in April-July 1976 in solar mini-

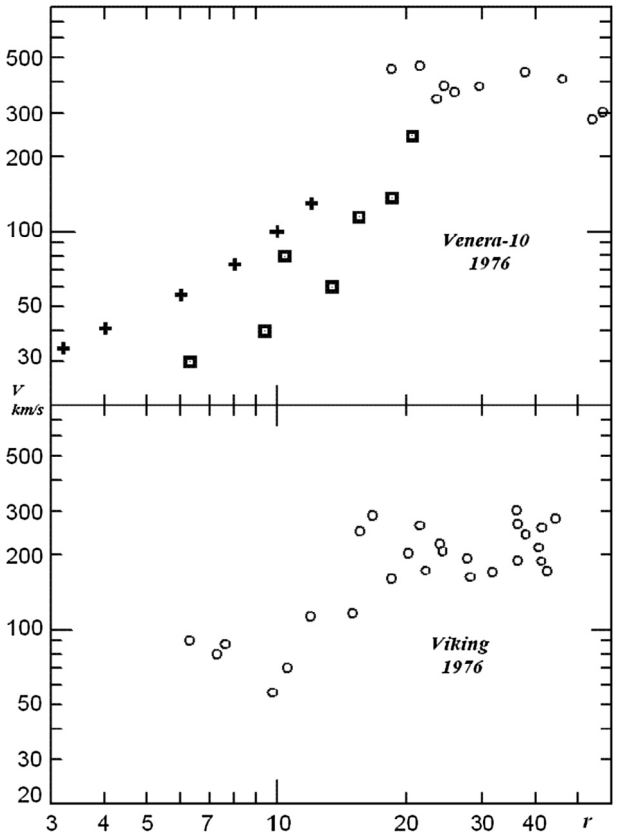

Fig. 2. Solar wind velocity (in km/s) experimental heliocentric distance dependencies in low solar activity. The heliocentric distance here and in the following is expressed in solar radii units. The results of the first method are marked by squares, the second – by triangles, the third – by circles, the fourth – by crosses.

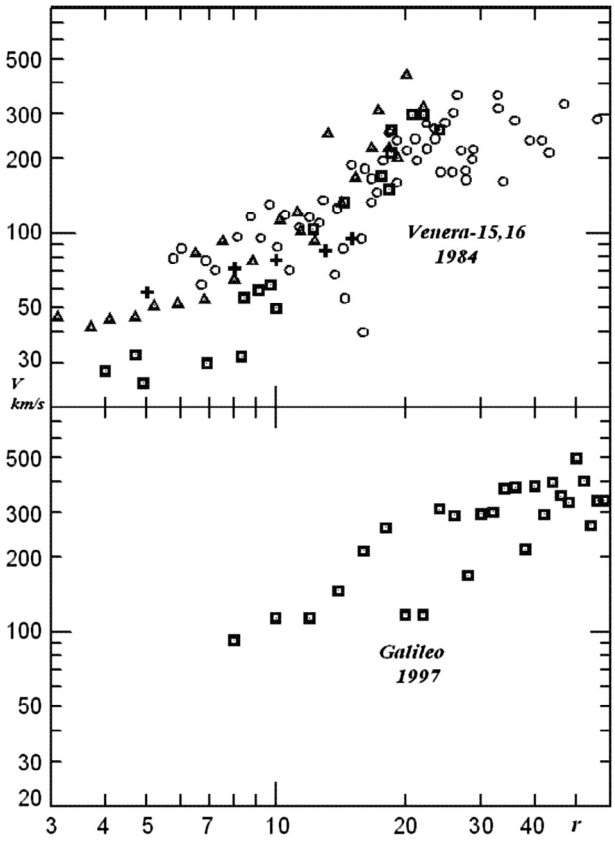

Fig. 3. Solar wind velocity (in km/s) experimental heliocentric distance dependencies in moderate solar activity. The results of the first method are marked by squares, the second – by triangles, the third – by circles, the fourth – by crosses.

mum. For the analysis chosen were 48 radio communication sessions, and the heliocentric distance varies from 58 to 3. To estimate the solar wind velocity the third method was applied when $18 < r < 58$, the first – when $6 < r < 21$, the fourth – when $3 < r < 12$.

From the graph one can see that there is no noticeable velocity variation at heliocentric distances $30 < r < 60$: the average solar wind velocity is equal to 380 ± 80 km s^{-1}. The velocity decreases at heliocentric distances $6 < r < 20$. At heliocentric distances $3 < r < 5$ the average solar wind velocity is equal to 42 ± 15 km s^{-1}.

Another solar wind velocity heliocentric distance dependence was obtained from radio signals of the "Viking" spacecraft (Tyler et al., 1981) in October 1976 – January 1977 in solar minimum. The information on amplitude fluctuations of radio signal at the wavelength λ_3 was used, and the heliocentric distance varied from 45 to 6. To estimate the solar wind velocity the third method was applied. The dependence (Tyler et al., 1981) is shown in the lower graph of Fig. 2. It is seen that the solar wind velocity varies in the interval $240 < V < 320$ km s^{-1} at heliocentric distances $24 < r < 40$, and it is equal to 74 ± 30 km s^{-1} at heliocentric distances $7 < r < 9$. The good conformity of "Venera-10" and "Viking" results at heliocentric distances $7 < r < 20$ testifies for strong increase of solar wind velocity with heliocentric distance. The data from both missions ("Venera-10" and "Viking") reveal an essentially constant solar wind velocity at heliocentric distances $30 < r < 50$.

A large amount of information was obtained from spacecraft "Venera-15" and "Venera-16" carried out at the decimeter wavelength λ_1 and the centimeter wavelength λ_2. To estimate the solar wind velocity all four methods mentioned above were applied. The use of many communication sessions along with two wavelengths and four methods to estimate the solar wind velocity enhances the reliability of the derived solar wind velocity heliocentric distance dependence (Efimov et al., 1987, 1990; Rubzov et al., 1987; Yalovlev et al., 1987; Yakovlev et al., 1988b, 1989; Yakubov et al., 1991) shown in the upper graph of Fig. 3. Similar to the upper graph of the Fig. 2 there is no noticeable velocity variation at heliocentric distances $36 < r < 50$: the average solar wind velocity is equal to 280 ± 50 km s^{-1}. The velocity decreases to the average value of 50 ± 20 km s^{-1} at heliocentric distances $4 < r < 6$. The use of different methods to measure the solar wind velocity provides the opportunity to estimate the precision of measurements: for $r > 16$ different methods lead to the same velocity value whereas for $r < 9$ the third (amplitude) method leads to the overestimated velocity value as against the first and the second (frequency) ones lead.

The solar wind velocity heliocentric distance dependence derived from the radio-sounding data of the "Galileo" spacecraft (at the wavelength λ_3) in January-February 1997 under moderate solar activity (Efimov et al., 2009) is shown in the lower graph of Fig. 3. The 7 first method was applied to estimate the solar wind velocity; frequency fluctuations registered at several long spaced ground stations were analyzed. Efimov et al. (2009) noted the solar wind velocity variability: the velocity varied from 160 km s^{-1} to 600 km s^{-1} during five hours. Therefore each point in the graph is the average over the interval ± 1 solar radius (that is, over 10–20 measurements of velocity) round the corresponding heliocentric distance shown on abscissa axis. As is easy to see there is no noticeable velocity variation at heliocentric distances $40 < r < 60$: the average solar wind velocity is equal to 370 ± 40 km s^{-1}. At heliocentric distances $7 < r < 30$ the velocity decreases and its average value is equal to 100 ± 30 km s^{-1} at heliocentric distances $8 < r < 10$.

Let us consider the solar wind velocity heliocentric distance dependence derived from the radio-sounding data of the "Ulysses" spacecraft (at the wavelengths λ_3 and λ_4) in August-September 1991 under high solar activity (Janardhan et al., 1999; Wohlmuth et al., 1997). To estimate the solar wind velocity the first method was applied in Janardhan et al. (1999), the second – in Wohlmuth et al. (1997). According to Janardhan et al. (1999), Wohlmuth et al. (1997) there was high dispersion of the solar wind velocities at small heliocentric distances. The analysis of the correlation function of frequency fluctuations registered at two spaced ground stations revealed

communication sessions when two correlation maxima existed (Chashei et al., 2005). Chashei et al. (2005) established that two values for the velocity had taken place on the ray path during the communication sessions. This could be interpreted as the simultaneous presence of two solar wind streams with different velocities on the ray path. The additional analysis (Efimov et al., 2003, 2005b) confirmed the high variability of the solar wind velocity. Let us note that because of the "Ulysses" spacecraft trajectory the solar wind velocities measured at heliocentric distances $r < 10$ refer to high heliolatitudes. Under high solar activity the average solar wind velocity was equal to 390 ± 100 km s^{-1} at heliocentric distances $23 < r < 34$, and 130 ± 40 km s^{-1} at heliocentric distances $7 < r < 8$.

Let us discuss the solar wind velocity heliocentric distance dependence at heliolatitudes below 60° for low and moderate solar activity. The main influence of the solar wind on the radio wave propagation is concentrated in the closest to the Sun part (r_0) of the ray path because of the solar wind plasma density decrease with heliocentric distance. This point permits to consider the heliocentric distance dependence of the solar wind velocity ($V(r_0)$) though the solar wind presents everywhere along the ray path. To approximate the solar wind velocity heliocentric distance dependence one can use the empirical equation:

$$V_a(r) = V_m \tanh(x) = V_m(e^x - e^{-x})(e^x + e^{-x})^{-1} \quad (5)$$

where $x = \eta r$, V_m – is the solar wind velocity at the Earth orbit ($r = 215$). For free parameter values $V_m = 300$ km s^{-1}, $\eta = 0.04$ Eq. (5) rather well describes the solar wind velocity heliocentric distance dependence at heliocentric distances $3 < r < 50$. The approximation refers to heliolatitudes below 60° for low and moderate solar activity. According to Jensen et al. (2016), Yalovlev et al. (1987), Yakovlev et al. (1988b) the solar wind sonic velocity is achieved at the heliocentric distance $12 < r_s < 14$, and the solar wind Alfvenic velocity – at the heliocentric distance $16 < r_a < 18$.

3. Solar wind density

First estimates of electron concentration near the Sun were derived from Thompson scattering of solar light on solar plasma environment electrons. The phenomenon was observed as K-corona by means of coronographs. Based on the observations the average spherically symmetric electron concentration heliocentric distance dependence was approximated by the power law:

$$N(r) = Ar^{-6} + Br^{-2} \quad (6)$$

where $A = 1.3 \cdot 10^8$ cm^{-3} and $B = 1.1 \cdot 10^6$ cm^{-3} at heliocentric distances $r > 2$.

Following the discovery of a pulsar situated approximately in the ecliptic plane, a novel method based on the measurement of the radio-wave group delay in plasma was utilized to estimate the electron concentration of the solar plasma environment (Weisberg et al., 1976, and references therein). One measures the difference in times of arrival of pulsar impulses on two frequencies that is proportional to the total electron content along the ray path. Assuming the spherically symmetric electron concentration distribution one estimates the electron concentration at several heliocentric distances with the help of the method. Troubles of the method are connected to strong interfering solar radio-frequency emission that prevents obtaining the electron concentration heliocentric distance dependence in the solar wind acceleration region.

The first solar wind density heliocentric distance dependence derived from radio sounding onboard spacecraft was published in Muhleman et al. (1977). Muhleman et al. (1977) exploited the single frequency communication line with the "Mariner-6" spacecraft and the "Mariner-7" one to measure the radio delay in plasma. The coherent response mode for modulated radio waves used in the experiments allows the determination of the Doppler frequency shift and the distance to the spacecraft with high precision. These data along with celestial mechanics allows the reconstruction of the spacecraft trajectory including the distance between the spacecraft and the ground station (Fig. 1). When the ray path approaches the Sun the apparent distance increase due to the radio delay in plasma appears. The delay is proportional to the double total electron content along the ray path. Radio sounding from "Mariner-6" and 'Mariner-7" spacecraft realized in April-May 1970 in solar minimum provided the electron concentration heliocentric distance dependence at heliocentric distances $4 < r < 14$. The dependence was supposed as follows:

$$N(r) = Ar^{-6} + Br^{-\xi} \quad (7)$$

and free parameters A, B, ξ were adjusted from radio-sounding experiments. According to the "Mariner-6" data $A = 0.69 \cdot 10^8$ cm^{-3}, $B = 0.54 \cdot 10^6$ cm^{-3}, $\xi = 2.05$, and $A = 1.3 \cdot 10^8$ cm^{-3}, $B = 0.66 \cdot 10^6$ cm^{-3}, $\xi = 2.08$ according to the "Mariner-7" data. From Eq. (7) one can estimate the electron concentration at the heliocentric distance $r = 10$ as $N = 5 \cdot 10^3$ cm^{-3}.

More reliable information on the solar wind density heliocentric distance dependence was collected with the help of dual-frequency communication line when trajectory data uncertainties weakly influenced on the total electron content. The dual-frequency technique allows measuring the difference between radio delays $\Delta t_{3,4}$ on two frequencies (namely, t_3 and t_4) when the ray path AB both approaches the Sun and moves away from the Sun. It is important to define $\Delta t_{3,4}$ as the differential group delay time, a quantity proportional to the absolute value of the total electron column density. This should be distinguished from the differential phase delay time, which yields only the changes in electron column density from the start of the measurements. The experimental curve $\Delta t_{3,4}(r_0)$ determines the total electron content J along the ray path AB that allows to derive the electron concentration heliocentric distance dependence N(r). According to Fig. 1 the impact parameter

(that is the closest approach to the Sun) of the ray path CO is equal to r_0 and the distance to the current point of the ray path – r_1. On high frequencies the plasma refraction coefficient is related to the electron concentration as $n = 1 - DNf^{-2}$, therefore the radio-wave delay in plasma is proportional to the total electron content:

$$\Delta t = Df^{-2}c^{-1}\int_A^B N(r)dl = Df^{-2}c^{-1}J(r_0) \tag{8}$$

As is easy to see (from Eq. (8)) the difference between radio delays $\Delta t_{3,4}$ measured on frequencies f_3 and f_4 is connected to the total electron content as follows:

$$J(r_0) = \frac{\Delta t_{3,4}(r_0)c}{D(f_3^{-2} - f_4^{-2})} \tag{9}$$

Here $D = 40.4\ m^3\ Hz^2$, c – is the speed of light in vacuum (in ms^{-1}), N – is the electron concentration (in m^{-3}), f – is the frequency (in Hz). Taking into account that the length element dl of the ray path AB is related to the heliocentric distance r as $dl = (r^2 - r_0^2)^{-1/2}2rdr$ one can write:

$$J(r_0) = 2\int_{r_0}^{CB} N(r)(r^2 - r_0^2)^{-1/2}rdr \tag{10}$$

In Eq. (10) the inessential approximation $CB \cong CA$ is accepted, that is the integral along the ray path AB is equal to the integral along the segment CB multiplied by 2 (Fig. 1). The total electron content is derived from the experimental data, but the goal is to determine the electron concentration heliocentric distance dependence N(r). The Abel integral transformation gives the rigorous solution of the problem:

$$N(r) = -\frac{1}{\pi}\int_r^{CB}\frac{dJ}{dr_0}\frac{dr_0}{(r^2 - r_0^2)^{1/2}} \tag{11}$$

The limited number of experimental points each measured with substantial errors yields the dependence $J(r_0)$ therefore it is difficult to find the derivation dJ/dr_0 from the experimental data. So one uses an appropriate approximation of the electron concentration heliocentric distance dependence N(r) and finds parameters of approximation from Eq. (10). For $r > 4$ the possible approximation is as follows:

$$N(r) = Br^{-\xi}F(\theta) \tag{12}$$

Here $F(\theta)$ is the model approximation of the electron concentration heliolatitude dependence (various according to various authors). If a spacecraft moves almost in the ecliptic (the heliolatitude is lower than 40°) one supposes $F = 1$. Eq. (12) has two sought parameters: B and ξ. As there is no solar wind velocity heliocentric distance dependence for $r > 30$ then one accepts $N(r) \sim r^{-2}$ and $\xi = 2$. However the solar wind velocity increases up to 5–7 times when the heliocentric distance increases from 7 to 25, so that ξ will differ from 2 in this heliocentric distance interval. Anderson et al. (1987), Bird et al. (1994, 1996), Krisher et al. (1991), Muhleman and Anderson (1981), Paetzold et al. (1995), Paetzold and Bird (1998), Woo (1996) find parameters B and ξ from experimental dependencies $J(r_0)$ by fitting.

Dual-frequency radio-sounding experiments of the solar plasma environment were realized onboard the "Viking" spacecraft that had the dual-frequency (f_3 and f_4) communication line (Muhleman and Anderson, 1981). Experiments were carried out in November-December 1976 in solar minimum when the difference between radio delays $\Delta t_{3,4}$ was measured in the impact parameter heliocentric distance interval $4 < r_0 < 170$ for the ray path AB both approached the Sun and moved away from the Sun. According to Muhleman and Anderson (1981) the experimental dependence $\Delta t_{3,4}(r_0)$ was well approximated as follows:

$$\Delta t_{3,4} = 1.2 \times 10^5 r^{-1.7} + 2.55 \times 10^4 r^{-1} \tag{13}$$

where $\Delta t_{3,4}$ was expressed in nanoseconds. On these grounds Muhleman and Anderson (1981) supposed the electron concentration heliocentric distance dependence approximation as follows:

$$N(r,\theta) = B_1 r^{-2.7}\exp\left(-\frac{\theta^2}{\theta_1^2}\right) + B_2 r^{-2} \tag{14}$$

Here θ is the heliolatitude. The exponential multiplier of first term describes the supposed heliolatitudinal decrease of electron concentration; under $\theta_1 = 8°$ and for $|\theta| < 40°$ it can be taken as unity. The best correspondence to the experimental data gives $B_1 = 1.32 \cdot 10^6\ cm^{-3}$, $B_2 = 2.3 \cdot 10^5\ cm^{-3}$. Another solar wind density heliocentric distance dependence was obtained with the help of Eq. (11). One calculated the derivative dJ/dr_0 numerically after averaging the experimental data $J(r_0)$ using the running window of the width $\Delta r = 2$. Both methods lead to the same result that testifies for the reliability of the calculated dependence N(r). According to the data $N = 6 \cdot 10^3\ cm^{-3}$ at $r = 10$ and $N = 10^3\ cm^{-3}$ at $r = 20$. The data quite well corresponds to the dependence $N(r) \sim r^{-2}$ for $r > 40$. The systematic excess of the data over the dependence $N(r) \sim r^{-2}$ is evident for $r < 20$ that testifies for the solar wind velocity decrease when the heliocentric distance decreases.

The results of measurements of $\Delta t_{3,4}$ and $J(r_0)$ from the solar plasma environment radio sounding onboard the "Voyager-2" spacecraft in November-December 1985 in solar minimum are presented in Anderson et al. (1987). The spacecraft was located near the ecliptic plane such that the ray path to the Earth remained below 8° at the proximate point to the Sun. The limited number of $\Delta t_{3,4}$ measurements in the impact parameter interval $6 < r_0 < 38$ were realized in the experiments. To derive the dependence N(r) Anderson et al. (1987) exploited Eq. (12) for $F(\theta) = 1$ and found the values of parameters B and ξ. It turned out that a strong asymmetry was observed for the solar wind density: for the ray path approach to the Sun it was found $\xi = 2.6$, $N(10) = 6 \cdot 10^3\ cm^{-3}$, whereas $\xi = 2$, $N(10) = 9.5 \cdot 10^3\ cm^{-3}$ when the ray path moved away

from the Sun. It was shown (Woo, 1996) with the help of coronograph observations that the asymmetry (the disparity in radial profiles) was caused by longitudinal variations stemming from probing of significantly different source regions. One more dual-frequency radio sounding was realized onboard the "Voyager-2" spacecraft in December 1988 in solar maximum (Krisher et al., 1991). The majority of delay measurements was conducted in the impact parameter interval $10 < r_0 < 87$ at heliolatitudes below 20°. After data processing based on Eq. (12) two pairs of parameter values were found, namely, $\xi = 2.08 \pm 0.05$, $B = (2.93 \pm 0.07) \cdot 10^6$ cm^{-3} and $\xi = 2.28 \pm 0.05$, $B = (7.08 \pm 0.24) \cdot 10^6$ cm^{-3}. Despite the lack of data for $r < 10$ the estimates $\xi = 2.7 \pm 0.2$, $B = (2.1 \pm 0.4) \cdot 10^7$ cm^{-3} at short heliocentric distances were derived. According to the experiments $N(10) = 3.4 \cdot 10^4$ cm^{-3} and $N(20) = 5.8 \cdot 10^3$ cm^{-3} that testifies for the strong enhancement of the electron concentration in solar maximum.

Radio sounding onboard the "Ulysses" spacecraft was realized in May-September 1991 in solar maximum (Bird et al., 1994; Paetzold et al., 1995). Fifty-six measurements of the delay $\Delta t_{3,4}$ were conducted in the impact parameter interval $r_0 = (40–5)$ at heliolatitudes below 20°. The total electron content at high heliolatitudes (where the heliolatitudinal dependence $F(\theta)$ should be taken into account) was determined in six experiments. Based on Eq. (12) for the ray path approach to the Sun it was found $\xi = 2.54 \pm 0.05$, $B = (3.61 \pm 0.04) \cdot 10^6$ cm^{-3}, whereas $\xi = 2.42 \pm 0.05$, $B = (2.26 \pm 0.03) \cdot 10^6$ cm^{-3} when the ray path moved away from the Sun; $N(20) = (1.7 \pm 0.1) \cdot 10^3$ cm^{-3}. Bird et al. (1994), Paetzold et al. (1995) noted irregular deviations from Eq. (12) and connected the deviations with solar active regions. One more radio sounding onboard the "Ulysses" spacecraft was realized in February-March 1995 (Bird et al., 1996; Paetzold and Bird, 1998). Near-polar solar plasma environment was sounded in the impact parameter interval $21 < r_0 < 30$ when the heliolatitude varied from $\theta = 30°$ to $\theta = 84°$. A coarse heliolatitude dependence of electron concentration was derived in Bird et al. (1994). Models from earlier work (Tyler et al., 1981; Muhleman and Anderson, 1981) were found to be poor representations of the latitude dependence.

Multiple measurements of electron concentration provided solar wind density heliocentric distance dependencies at heliolatitudes below 40° under various solar activity levels. These do not demonstrate any clear solar activity dependence of the average electron concentration. For the average electron concentration one can accept $N(20) = 1.4 \cdot 10^3$ cm^{-3} and $N(10) = 6.7 \cdot 10^3$ cm^{-3}. The radial falloff exponent varies from 2.05 to 2.6; the closer is the ray path to the Sun, the greater is radial falloff exponent. The comparison of electron concentration heliocentric distance dependencies derived from both radio sounding and Thompson scattering demonstrated the concordance of data sets obtained by different methods in the heliocentric distance interval $3 < r < 6$. The detailed comparison between heliocentric distance dependencies N(r) obtained by radio sounding and Thompson scattering is given in Yakovlev (2002), Jensen et al. (2016). The comparison shows good correspondence between the two techniques for $3 < r < 5$, but for $6 < r < 25$ the distinction takes place, and it is natural because the Allen-Baumbach traditional models worse describe experimental data of radio sounding. The flow through the solar centered sphere:

$$L = 4\pi r^2 NV = 4\pi (215)^2 N_m V_m \tag{15}$$

(where N_m – is the electron concentration at the Earth orbit) along with Eq. (5) gives:

$$N_a = N_m (215)^2 [r^2 \tanh(x)]^{-1} \tag{16}$$

Eq. (16) is valid in case of constant L and no heliolatitude dependencies of solar wind velocity and electron concentration. According to Eq. (16) the electron concentration decreases with heliocentric distance as $N(r) \sim r^{-2}$ for $r > 40$ where the solar wind velocity does not depend on heliocentric distance. Electron concentrations calculated from Eq. (16) under the parameters $N_m = 8$ cm^{-3} and $\eta = 0.04$ are in satisfactory agreement with experimental data under low solar activity. Due to the solar wind changeability Eq. (16) gives approximate values of N: N(10) variates within 30% under moderate solar activity but in case of CME N(10) enhances sometimes up to three times.

4. Power and acceleration of the solar wind

Let us calculate the power and the acceleration of the solar wind from Eqs. (5) and (16).

The solar mass loss due to the solar wind is as follows:

$$\frac{dM}{dt} = 4\pi r^2 m V(r) N(r) \tag{17}$$

where m – is the proton mass. According to radio sounding the average solar wind velocity can be estimated as $V = 100$ km s^{-1} and the average electron concentration - $N = 7 \cdot 10^3$ cm^{-3} at the heliocentric distance $r = 10$. From Eq. (17) one calculates $dM/dt = 0.7 \cdot 10^9$ kg s^{-1}. At the Earth orbit ($r = 215$) in case of $V = 300$ km s^{-1} and $N = 8$ cm^{-3} one calculates from Eq. (17) $dM/dt = 1.1 \cdot 10^9$ kg s^{-1}.

The total power of the solar wind is as follows:

$$W = \frac{dM}{dt}\frac{V^2}{2} \tag{18}$$

After the substitution of Eqs. (5) and (17) into Eq. (18) one calculates:

$$W = \frac{dM}{dt}\frac{V_m^2}{2}\tanh^2(x) \tag{19}$$

The heliocentric distance dependence of the solar wind power plotted from Eq. (19) is shown in Fig. 4 as number 1. As is easy to see the solar wind power is enhanced approximately thirty times when the heliocentric distance increases from 6 to 30.

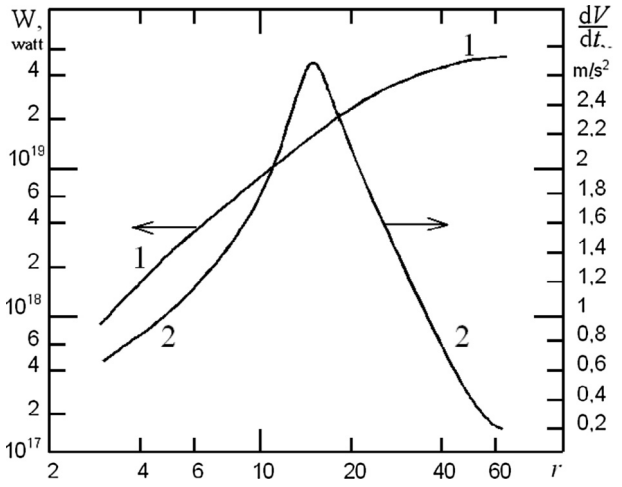

Fig. 4. Power W and acceleration dV/dt in the solar wind acceleration region.

The solar wind acceleration is as follows:

$$\frac{dV}{dt} = \frac{dV}{dr}\frac{dr}{dt} = \frac{dV}{dr}V \tag{20}$$

From Eq. (5) one calculates:

$$\frac{dV}{dt} = 4\eta\frac{V_m^2}{R}\frac{\tanh(x)}{(e^x + e^{-x})^2} \tag{21}$$

Here R is the solar radius, $4\eta V_m^2/R = 20.6\ \mathrm{ms}^{-2}$ for $\eta = 0.04$, $V_m = 300\ \mathrm{km\ s}^{-1}$. The heliocentric distance dependence of the solar wind acceleration plotted from Eq. (21) is shown in Fig. 4 as the number 2. As is easy to see the maximum of the acceleration ($2.7\ \mathrm{ms}^{-2}$) is achieved at $r = 15$. Real changes of V(r) and N(r) along with methodic errors lead to uncertainties of averaged approximations, represented by Eqs. (5) and (16), so Eqs. (19) and (20) as well as numerical values of solar wind power and acceleration, shown on Fig. 4, are approximations too.

5. Temporal spectra of frequency and amplitude fluctuations

It is possible to derive statistical characteristics of irregularities of solar wind plasma environment from temporal spectra parameters of electron concentration fluctuations, which, in turn, can be determined from measurements of temporal spectra of radio frequency and amplitude fluctuations.

The determination of amplitude fluctuation spectra $G_a(F)$ is possible within narrow limits. For the fluctuation frequency $F > 20$ Hz the spectral intensity G_a is usually small and it is difficult to separate it from noise fluctuations. For $F < 0.3$ Hz the determination of the spectral intensity G_a is impeded because of enhancement of variations of the complicated system of the signal receiver. It has been possible to obtain the plausible amplitude spectra for frequency interval between 0.3 Hz and 20 Hz. In the small range of fluctuation frequencies F the spectrum of amplitude fluctuations can be expressed as the power-law dependence $G_a \propto F^{-\chi_a}$, where χ_a is the spectral index of amplitude fluctuation spectrum. Also it is possible to find the spectrum of frequency fluctuations for wider range of fluctuation frequencies. In this wider interval of fluctuation frequencies F the spectrum density $G_f(F)$ can also be expressed as the power-law dependence $G_f \propto F^{-\chi_f}$, where χ_f is the spectral index of temporal spectrum of frequency fluctuations.

Many spectra $G_f(F)$ and $G_a(F)$ were obtained at various heliocentric distances by radio sounding. From these data one can derive the information on the plasma turbulence with the help of the theory of radio wave propagation in statistically inhomogeneous medium. According to the theory the spectrum of refraction coefficient fluctuations $G_n(q)$ is expressed as follows:

$$G_n(q) = C^2(q_0^2 + q^2)^{-p/2}\exp\left(-\frac{q^2}{q_m^2}\right) \tag{22}$$

Here p is the spectral index characterizing the turbulence regime of medium, $q = 2\pi/l$ is the spatial wave number corresponding to inhomogeneities of the scale l, $q_0 = 2\pi/l_{max}$ is the wave number corresponding to the outer (maximum) spatial scale l_{max}, $q_m = 2\pi/l_{min}$ is the wave number corresponding to the inner spatial scale l_{min}. It is expected that the outer scale l_{max} has the order of solar radius, while the inner one l_{min} is small and characterizes the process of turbulence energy transportation into the heat of medium. It is known that under both fragmentation of turbulence vortexes in terrestrial atmosphere and random mixing of plasma streams or liquid ones the Kolmogorov spectrum with $p \cong 11/3$ is often realized. The multiplier C characterizes the medium inhomogeneity intensity and is connected to the dispersion of refraction coefficient fluctuations σ_n^2. If the registration of medium inhomogeneties is experimentally possible for scales $l_{min} < l < l_{max}$, the spectrum of refraction coefficient fluctuations can be described as follows:

$$G_n = C^2 q^{-p} \tag{23}$$

Eqs (22) and (23) are phenomenological representations of plasma statistical inhomogeneities. Certainly these do not describe "true" turbulence of medium but rather the spectrum of plasma statistical inhomogeneities of various origin, such as inhomogeneities elongated along the magnetic field, small ejections of plasma, filamentary structures. Let us note that Eq. (23) is chosen by analogy with a neutral gas and its application to the description of solar plasma environment inhomogeneities in the magnetic field has no theoretical substantiation. The technique of radio sounding allows to investigate plasma statistical inhomogeneities, which cause radio fluctuations. The representation of the spectrum of these fluctuations as Eq. (22) is phenomenological, but nevertheless it allows to determine four quantitative characteristics of statistically inhomogeneous medium. Certainly the usage of the term "turbulence" to describe statistical inhomogeneities of various

origin is non-rigorous, but the rigorous theory of turbulence of magnetized plasma is still under development. Radio fluctuations are stipulated by the influence of plasma refraction coefficient statistical inhomogeneities δn connected to electron concentration fluctuations δN through the equation:

$$\delta n = -40.4 f^{-2} \delta N \tag{24}$$

where δN is measured in m^{-3} and f – in Hz. As is easy to see from Eq. (24) spatial spectra of refraction coefficient G_n and electron concentration G_N are identical. Ishimaru (1978) gave the general theoretical analysis of radio fluctuations in statistically inhomogeneous medium, while Armand et al. (1987), Armstrong and Woo (1981), Woo (1978), Woo et al. (1976a, 1976b), Bird (1982), Bird and Edenhofer (1990), Yakovlev (2002) applied the theory to the analysis of radio frequency and amplitude fluctuations in the solar wind. They took into account the heliocentric distance dependence of parameters of the spectrum (22) and accepted a few essential hypotheses. They supposed that plasma inhomogeneities situated on the ray path AB could be presented as the relatively thin "phase screen" D_1D_2 centered at the point C while parameters of the spectrum $G_n(q)$ depended only on the distance r_0 between the solar center O and the point C. Under such assumptions the shaded region along the segment D_1D_2 (which delivers the main deposit to the radio fluctuations) is situated at the heliocentric distance r_0 and the "phase screen" thickness is approximately equal to r_0 (Fig. 5). This model of "phase screen" has no distinctions between r_0 and r. Inhomogeneities were also considered as "frozen" into the solar wind (moving with the velocity V), and were assumed isotropic though real inhomogeneities were radial elongated due to the magnetic field influence.

The ray path AB moves in the medium with the velocity $V_1 = V \pm dr_0/dt$, where V is the solar wind velocity, dr_0/dt is the velocity of approach of the ray path to the Sun (spacecraft' recess behind the Sun – sign "plus") or its motion away from the Sun (sign "minus"). Usually $V > dr_0/dt$ for $r > 8$ and one can suppose $V_1 \cong V$. The ray path intersects irregularities with the scale l during the time $\Delta t = l/V$ therefore the fluctuation frequency F can be estimated as $F \cong V/l$. The low frequency part of the frequency fluctuation spectrum is determined by the effect of large-scale plasma irregularities adjacent to the outer turbulence scale l_{max}, while high-frequency fluctuations depend on small-scale plasma irregularities with the scales exceeding the inner scale of turbulence l_{min}. Armand et al. (1987), Armstrong and Woo (1981), Woo (1978), Woo et al. (1976a, 1976b), Yakovlev (2002) showed that radio amplitude fluctuations arose mainly from small-scale plasma inhomogeneities of the scale of the order of first Fresnel zone diameter $l_\varnothing$, and the frequency spectrum of radio amplitude fluctuations $G_a(F)$ can be limited as follows:

$$V_1/l_\varnothing \geqslant F > V_1/l_{min} \tag{25}$$

where $l_\varnothing$ is the first Fresnel zone diameter

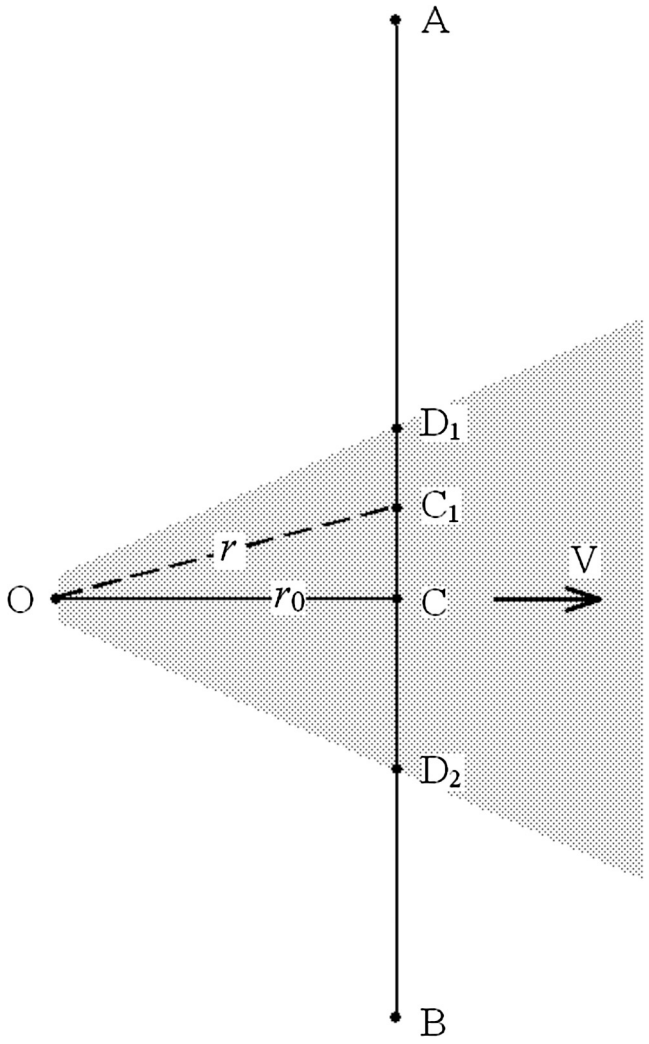

Fig. 5. Outline of plasma turbulence research.

$$l_\varnothing = 2\left(\frac{\lambda l_1 l_2}{l_1 + l_2}\right)^{1/2} \tag{26}$$

where $l_1 = AC$ is the distance between the spacecraft and the point of the ray path closest approach to the Sun, $l_2 = BC$ is the distance between the ground station and the point of the ray path closest approach to the Sun (Fig. 5). The theory of amplitude fluctuations is valid for weak fluctuations when the standard deviation $\sigma_a < 0.6$. Fluctuations of frequency f arise mainly from large scale plasma inhomogeneities and its spectrum $G_f(F)$ has the maximum on low frequencies

$$V_1/l_{max} > F \geqslant V_1/l_\varnothing \tag{27}$$

The theory of frequency fluctuations is valid for both weak and strong fluctuations.

If temporal experimental spectra of amplitude and frequency fluctuations are obtained at the fulfillment of Eqs. (25) and (27) then it is possible to use Eq. (23) for the spatial spectrum of refraction coefficient of irregularities $G_n(q)$ at the theoretical analysis of these spectra. In this case both

the amplitude fluctuation spectrum and the frequency fluctuation spectrum can be presented by the power-law functions:

$$G_a = D_a F^{-\chi_a},\ \chi_a = p - 1 \quad (28)$$

$$G_f = D_f F^{-\chi_f},\ \chi_f = p - 3 \quad (29)$$

The spectral indexes of temporal spectra of amplitude fluctuations χ_a and frequency fluctuations χ_f depend on the spectral index p of plasma density turbulence. Multipliers D_a and D_f depend on the radio frequency f, the index of power p, and the heliocentric distance r.

Exploring radio fluctuations in the solar plasma environment one can obtain experimental spectra (28) and (29), find the value of p, and determine dispersions of amplitude fluctuations σ_a^2 and frequency fluctuations σ_f^2. The dispersions are determined by integration as follows:

$$\sigma^2 = \int_{F_{min}}^{F_{max}} DF^{-\chi} dF \quad (30)$$

where F_{max} and F_{min} are maximal and minimal frequencies of radio fluctuations for which experimental spectra $G_a(F)$ and $G_f(F)$ are available. To determine plasma turbulence characteristics one should obtain experimental spectra $G_a(F)$ and $G_f(F)$ as well as dispersions σ_a^2 and σ_f^2 in the variation interval of F as wide as possible for various heliocentric distances.

6. Spatial spectrum of plasma inhomogeneities

The heliocentric distance dependence of the index of power p can indicate the turbulence regime change in the solar wind formation region.

The validity of presentation of spectra $G_a(F)$ and $G_f(F)$ as power-law functions in the solar wind acceleration region was ascertained in radio-sounding experiments onboard "Mars-2" (1972) and "Mars-4" (1974) spacecraft. It was shown that the spectra could really be described by Eqs. (28) and (29), and the index of power p was estimated. The heliocentric distance dependence of the index of power p was revealed in radio-sounding experiments onboard the "Venera-10" spacecraft (1976): based on spectra $G_a(F)$ and $G_f(F)$ it was shown that within errors of measurement the index of power p corresponded to the Kolmogorov spectrum ($p = 11/3$) for heliocentric distances $20 < r < 55$ and p decreased for $r < 9$. The estimates of the index of power p described in Kolosov et al. (1982), Yakovlev et al. (1977) were derived from the data on the wavelength λ_1 of the deep space radio-communication system. Two research groups obtained estimates of p by the analysis of spectra of amplitude fluctuations and phase fluctuations, and by radio spectral line broadening in radio-sounding experiments onboard the "Viking" spacecraft (1976) from the data on the wavelength λ_3 of the deep space radio-communication system. The detailed analysis of fluctuating signals along with a great number of radio transmission sessions allowed deriving the reliable heliocentric distance dependence of p (Armstrong and Woo, 1981; Tyler et al., 1981). The heliocentric distance dependence of index of power of spatial spectrum of plasma inhomogeneities is shown in Fig. 6A (Armstrong and Woo, 1981). "Venera-15" and "Venera-16" spacecraft emitted radio waves at the wavelengths λ_1 and λ_2 and this allowed deriving the heliocentric distance dependence of p from amplitude fluctuation spectra for heliocentric distances $3 < r < 60$ (Efimov et al., 1987; Yakovlev et al., 1988b). The dependence is shown in Fig. 6B. Radio sounding onboard the "Galileo" (1999) spacecraft allowed deriving the heliocentric distance dependence of p from the analysis of spectra of radio frequency fluctuations at the wavelength λ_3 (Efimov et al., 2005a). The dependence is shown in Fig. 6C. Similar heliocentric distance dependencies were obtained in radio-sounding experiments onboard subsequent spacecraft (Chashei et al., 2005; Efimov et al., 2010a, 2010b).

Studies of spectra of radio fluctuations showed that the value of p corresponds to the Kolmogorov spectrum ($p = 3.66$) for $r \geq 25$ and the average value of $p = 3.0 \pm 0.2$ for

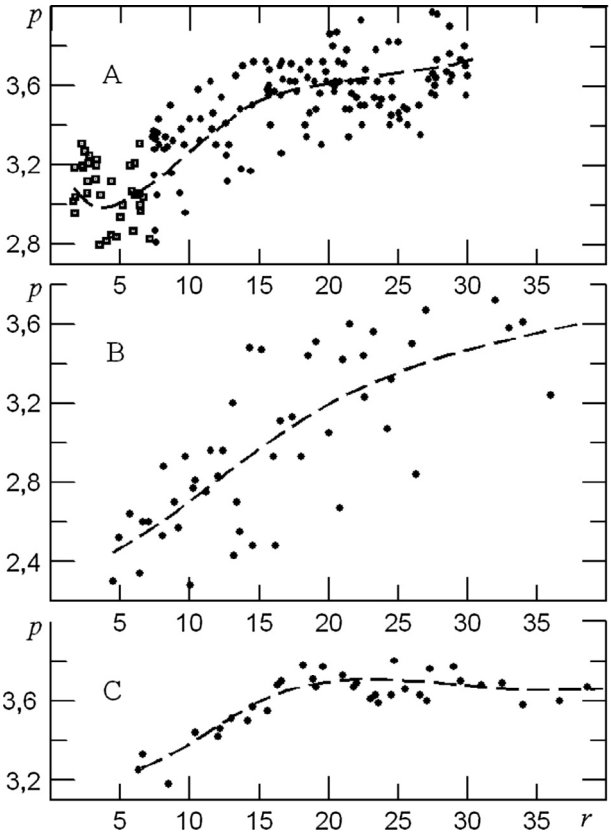

Fig. 6. Plasma inhomogeneity spectral index (p) heliocentric distance dependencies. The heliocentric distance dependence of p derived by Armstrong and Woo (1981) is shown in A. The heliocentric distance dependence of p derived from amplitude fluctuation spectra for heliocentric distances $3 < r < 60$ obtained from "Venera-15" and "Venera-16" data (Efimov et al., 1987; Yakovlev et al., 1988b) is shown in B. The heliocentric distance dependence of p derived from spectra of radio frequency fluctuations at the wavelength λ_3 obtained from "Galileo" data (Efimov et al., 2005a) is shown in C.

$3 < r < 5$. Fig. 6 testifies for the plasma turbulence regime change at heliocentric distances $5 < r < 18$ where the main acceleration of the solar wind takes place and its stream structure can already be formed (Pisanko, 1996) so that the beam instability created due to the interaction between solar wind streams with different velocities can be expected.

To determine the outer scale l_{max} of plasma inhomogeneities one should obtain experimental spectra of radio fluctuations for ultra low frequencies F. It is possible in the registration of high stable signals during a long time interval: only the registration of frequency fluctuations during long time intervals allows to obtain reliable low frequency spectra $G_f(F)$. In experiments onboard "Galileo" (1995) and "Ulysses" (1991) spacecraft the continuous registration of frequency fluctuations during more than 10 h took place, and this allowed to obtain spectra $G_f(F)$ reliable in the frequency range from $F \cong 10^{-1}$ Hz to $F \cong 3 \cdot 10^{-5}$ Hz (Chashei et al., 2007; Efimov et al., 2002b, 2010c; Ramzanov et al., 1979). The peculiarities of the spectra are the maximum of $G_f(F)$ at $F \cong 10^{-4}$ Hz and the decrease of $G_f(F)$ at lower frequency of fluctuations. The maximum of $G_f(F)$ exists at very low fluctuation frequency according to Eq. (22) and corresponds to the frequency (Efimov et al., 2002b):

$$F_{min} = Vl_{max}^{-1}\left(\frac{2}{p-3}\right)^{1/2} \tag{31}$$

Chashei et al. (2007), Efimov et al. (2010c) note that from Eq. (31) one can estimate the outer scale l_{max} from known velocity, index of power p and experimental value of F_{min}. The heliocentric distance dependence of l_{max} is shown in Fig. 7; points correspond to "Galileo" spacecraft (1995) signals, squares – to "Ulysses" (1991) ones. Despite the wide spacing of l_{max} the averaged heliocentric distance dependence of l_{max} can be indicated as follows:

$$l_{max}\ [\text{km}] \cong 1.2 \times 10^5 r$$

It is shown by the dashed line in Fig. 7; for $r = 10$ $l_{max} = 1.5 \cdot 10^6$ km, for $r = 25$ $l_{max} = 3 \cdot 10^6$ km. The outer scale is determined by the large-scale spatial structure of the solar corona, i.e. it is of the order of solar diameter.

To study small-scale plasma inhomogeneities one should explore experimental spectra of radio fluctuations on sufficiently high frequencies F. To determine the inner scale l_{min} exploited were experimental data on spectra of amplitude fluctuations and frequency fluctuations as well as the radio spectral line broadening when fluctuating signals on frequencies $F > 10$ Hz were registered. First, radio spectral line λ_1 broadening from the "Venera-10" spacecraft (1976) was exploited (Ramzanov et al., 1979). Ramzanov et al. (1979) showed that the spectral line shape contained new information on small-scale irregularities under large deviations δf from the line central frequency. Using the maximum frequency deviation (F_{max}) from the line central frequency it is possible to estimate the minimum scale of irregularities $l_{min} = V_1 F_{max}^{-1}$; the heliocentric distance dependence of l_{min} is depicted by squares in Fig. 8.

Frequency fluctuations under high frequency F were measured in radio-sounding experiments onboard the "Nozomi" (2000) spacecraft and reliable spectra $G_f(F)$ along with F_{max} were obtained (Efimov et al., 2010c). To determine G_{min} Efimov et al. (2010c) used the solar wind velocity V measured onboard other spacecraft. The values of l_{min} obtained in Efimov et al. (2010c) are depicted by tri-

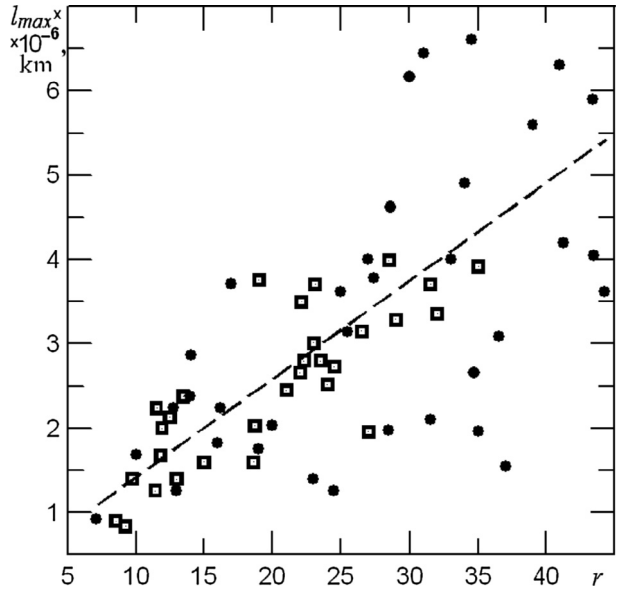

Fig. 7. Outer scale of plasma turbulence l_{max} at various heliocentric distances. Filled circles correspond to data obtained with the "Galileo" spacecraft (1995); open squares to "Ulysses" (1991).

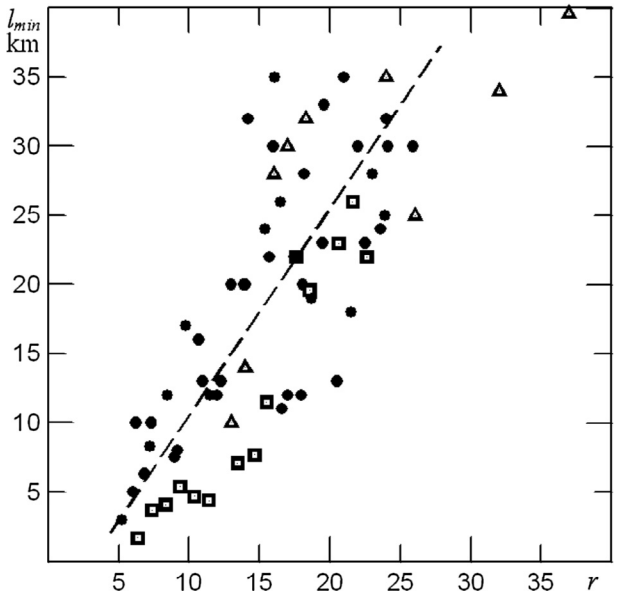

Fig. 8. Inner scale of plasma turbulence l_{min} at various heliocentric distances. The values of l_{min} are shown as open squares (Ramzanov et al., 1979), open triangles (Efimov et al., 2010c), and filled circles (Yakovlev et al., 1988b). The averaged heliocentric distance dependence is shown as a dashed line.

angles in Fig. 8. Another way to determine l_{min} was the analysis of amplitude fluctuations in radio-sounding experiments onboard "Venera-15" and "Venera-16" (1984) spacecraft (Yakovlev et al., 1988b). Registered were amplitude fluctuations at wavelengths λ_1 and λ_2. Under the arbitrary assumption that the spectral intensity G_a of for sure registered maximal frequency F_{max} is a hundred time smaller than registered at low frequency one Yakovlev et al. (1988b) find l_{min} from known V. The values of l_{min}, obtained in Yakovlev et al. (1988b), are depicted by points in Fig. 8. It is clear from Fig. 8 that various methods give close values of the turbulence inner scale l_{min}: for $r = 10$ $l_{min} = 13$ km, for $r = 20$ $l_{min} = 26$ km. The averaged heliocentric distance dependence

$$l_{\min}\ [\mathrm{km}] \cong 1.3r \tag{32}$$

is shown by dashed line in Fig. 8. The turbulence inner scale is of the order of proton gyroradius. It seems that the proton gyroradius is the minimal inhomogeneity scale where turbulence energy transfers into solar wind additional heating.

7. Radial variation of radio fluctuation intensity and fractional density Fluctuations

To understand the solar wind strong acceleration it is desirable to ascertain the plasma relative inhomogeneity heliocentric distance dependence. Let us characterize the radio fluctuation intensity by standard deviations of amplitude σ_a and frequency σ_f while the plasma relative inhomogeneity – by the ratio of electron concentration standard deviation σ_N to electron concentration value $\gamma = \sigma_N/N$ - amplitude of the fractional density fluctuation. Parameters σ_a, σ_f, σ_N are connected and depend on heliocentric distance.

Let us analyze experimental heliocentric distance dependencies of σ_a and σ_f. During radio sounding the frequency is always registered every second and only in selected space missions the amplitude was registered (15–30) times per second. σ_a and σ_f are calculated from these data. Various experimental heliocentric distance dependencies of σ_a are published in Efimov et al. (1987, 2008a), Kolosov et al. (1978), Rubzov et al. (1987), Yakovlev et al. (1980b, 1988a, 1988b), while heliocentric distance dependencies of σ_f – in Armand et al. (1988), Efimov et al. (1977, 2002a, 2008b, 2010a, 2010b, 2013, 2014), Kolosov et al. (1978), Yakovlev et al. (1980b). The authors of listed papers used power-law functions to fit experimental dependencies σ_a and σ_f:

$$\sigma_a \propto r^{-\alpha} \tag{33}$$

$$\sigma_f \propto r^{-\beta} \tag{34}$$

and determined the values of parameters α and β. In the listed above publications presented were experimental heliocentric distance dependencies of σ_a and σ_f that were obtained in six cycles of coronal radio-sounding experiments. The average $\alpha = 1.75 \pm 0.15$ for heliocentric distances $6 < r < 30$ was obtained from the amplitude data while the average $\beta = 1.70 \pm 0.17$ for heliocentric distances $5 < r < 40$ – from frequency data.

The determination of heliocentric distance dependence of amplitude of the fractional density fluctuation $\gamma(r)$ needs the electron concentration standard deviation heliocentric distance dependence $\sigma_N(r)$, which can be found from amplitude fluctuations or frequency fluctuations. As shown theoretically in Armand et al. (1987), Armstrong and Woo (1981), Efimov et al. (1977), Woo (1978), Woo et al. (1976a, 1976b), Yakovlev (2002) the determination of $\sigma_N(r)$ from $\sigma_a(r)$ faces difficulties. $\sigma_f(r)$ is more informative: it works for both strong and weak fluctuations covering longer heliocentric distance interval. One can determine $\sigma_f(r)$ both by the integration of spectra of frequency fluctuations (Eqs. (29) and (30)) and from the width of radio spectral line broadening $\Delta f \cong 2.5\sigma_f$.

Theoretical approximations of the relationship between σ_f and σ_N are published in Armand et al. (1987), Kolosov et al. (1982), Woo (1978), Yakovlev (2002). More convenient expression is presented in Efimov et al. (2010a, 2008b):

$$\sigma_f \propto \sigma_N \left[\left(\frac{\chi_f}{1-\chi_f} \right)^{1/2} L_e^{1/2} l_{\max}^{-\chi_f/2} V^{(\chi_f+1)/2} \right] \tag{35}$$

where $L_e \cong r_0 \cong D_1 D_2$ is the thickness of conventional phase screen, χ_f is the index of spectrum of frequency fluctuations, V is the velocity of plasma inhomogeneity transfer through the ray path, l_{max} is the outer scale of inhomogeneities. If we do not take into account cumbersome multipliers, which have no heliocentric distance dependence, put $L_e \cong r_0$, $\chi_f = p\text{-}3$, exploit experimental heliocentric distance dependence $l_{max}(r)$ and Eq. (34) for σ_f, then according to Eq. (35) we obtain:

$$\sigma_N \propto r^{-\beta} \left[\left(\frac{p-3}{4-p} \right)^{-1/2} r^{(p-4)/2} V^{(2-p)/2} \right] \tag{36}$$

According to Fig. 6 the index of spectrum of plasma spatial inhomogeneities p has weak heliocentric distance dependence for $15 < r < 40$, therefore let us put $p = 3.5$. Accepting the average value $\beta = 1.7$ one obtains (from Eq. (36)):

$$\sigma_N \propto r^{-1.95} V^{-1.75} \tag{37}$$

Eq. (37) is valid when σ_f is determined from very long records of frequency fluctuations. If σ_f is determined from a twenty or thirty minute record of frequency fluctuations, then the heliocentric distance dependence of l_{max} does not manifest itself and one should put $l_{max} = \text{const}$ that leads (from Eq. (35)) to:

$$\sigma_N \propto r^{-2.2} V^{-1.75} \tag{38}$$

According to Eqs. (5) and (16) $V = \text{const}$ and $N \propto r^{-2}$ for $r > 20$ so that the amplitude of the fractional density fluctuation γ will be almost constant for $15 < r < 30$ owing to Eqs. (37) and (38). Eqs (37) and (38) imply that the mean frequency deviation has a slightly different radial falloff, depending on the specific band in the fluctuation spectrum. The longer period fluctuations decrease more rapidly with r than the shorter period fluctuations. To determine the amplitude of the fractional density fluctuation γ in the solar wind acceleration region numerical calculations are needed to take into account heliocentric distance dependencies V(r), N(r), p(r). Calculations showed that the amplitude of the fractional density fluctuation γ increased with heliocentric distance in the solar wind acceleration region. The calculation is based on Eqs. (5) and (16) under $\beta = 1.7$. Experimental values of β varied from 1.5 to 1.9 for various space missions therefore various heliocentric distance dependencies of amplitude of the fractional density fluctuation (from almost independence on heliocentric distance till the increase with the heliocentric distance) could be realized. Estimates of amplitude of the fractional density fluctuation heliocentric distance dependencies derived from heliocentric distance dependencies of frequency fluctuations $\sigma_f(r)$ and amplitude ones $\sigma_a(r)$ under various assumptions about solar wind density heliocentric distance dependence N(r) and solar wind velocity one V(r) in various years are collected in Chashei et al. (2007), Efimov et al. (1977), Imamura et al. (2014), Rubzov et al. (1987), Woo et al. (1995), Yakovlev et al. (1988b). Let us note that heliocentric distance dependencies of amplitude of the fractional density fluctuation are doubtful for both $r < 5$ where radio fluctuations are large and $r > 40$ where the fluctuations are small; according to the publications values of γ variate strongly at small heliocentric distances and at large ones. Inside the heliocentric distance interval $6 < r < 40$ the dispersion of amplitude of the fractional density fluctuation remains acceptable. Heliocentric distance dependencies of amplitude of the fractional density fluctuation obtained from radio-sounding experiments (Imamura et al., 2014; Rubzov et al., 1987; Yakovlev et al., 1988b) onboard "Venera-15" and "Venera-16" spacecraft (1984) and onboard the "Akatsuki" spacecraft (2011) are shown in Fig. 9. Points and triangles in Fig. 9 correspond to frequency and amplitude data from "Venera-15" and "Venera-16" while crosses – to frequency data from "Akatsuki". The amplitude of the fractional density fluctuation γ (r) increase with heliocentric distance is evident: $\gamma = 0.08$ for r = (15–6) while $\gamma = 0.2$ for r = (30–20). Amplitude of the fractional density fluctuation values obtained from radio-sounding experiments (Chashei et al., 2007; Efimov et al., 1977) onboard the "Venera-10" spacecraft (1978) and the "Galileo" spacecraft (1997) are shown in Fig. 10. One can see the heliocentric distance independence (within errors of measurements) of amplitude of the fractional density fluctuation: its average value is equal to $\gamma = 0.25$. Woo et al. (1995) concluded that the fractional density fluctuation γ(r) was (a) essentially independent of heliocentric distance in the slow solar wind, and (b) was a factor thirty smaller in the fast wind than in the slow wind and increased dramatically with heliocentric distance.

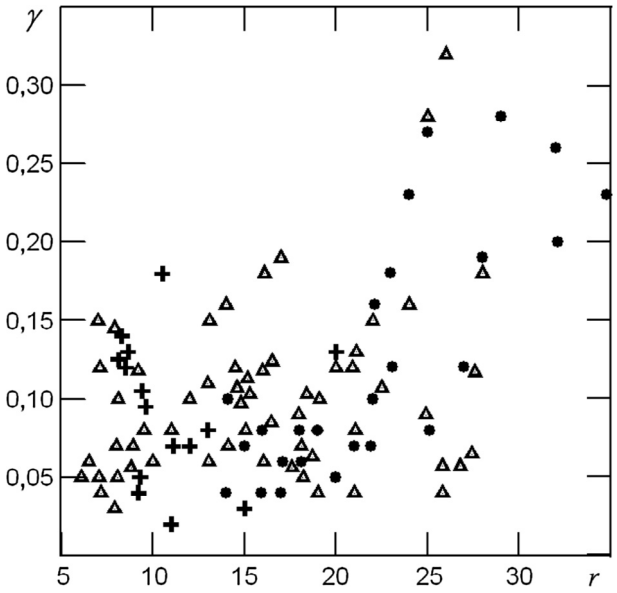

Fig. 9. Low values of fractional density fluctuations γ for $5 < r < 20$. Filled circles and open triangles correspond to frequency and amplitude data, respectively, from "Venera-15" and "Venera-16"; crosses correspond to frequency data from "Akatsuki".

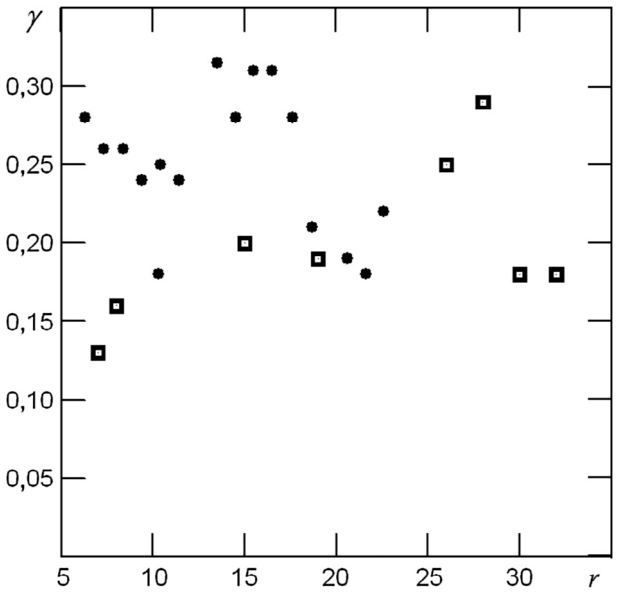

Fig. 10. High values of fractional density fluctuations in the solar wind acceleration region. Filled circles correspond to data from "Venera-10"; open squares to "Galileo".

8. Conclusions

An overview of coronal radio-sounding data is presented, applicable to heliocentric distances $3 < r < 60$, heliolatitudes below 60°, and minimum to moderate solar activity.

The heliocentric distance dependence of the solar wind velocity is presented in Section 2. The accuracy of the mean radial dependence, based on data from four space missions, is estimated to be less than 20%. There is not enough data at heliocentric distances below 4, where the error increases to about 40%. Eq. (5) is a satisfactory approximation to the solar wind heliocentric distance dependence for $r > 3$. The main acceleration of the solar wind takes place at heliocentric distances $7 < r < 24$, over which the solar wind velocity increases by a factor of seven.

The electron density decreases as r^{-2} at heliocentric distances $r > 24$, but falls off more rapidly closer to the Sun. Assuming conservation of solar wind flux, a satisfactory approximation for the heliocentric distance dependence of the electron density at $r > 3$ is given by Eq. (16).

Using Eqs. (5) and (16), it may be concluded that the solar wind power increases by a factor of 30 over the radial distance from 6 to 30; the maximum acceleration of 2.6 m s^{-2} is achieved at the heliocentric distance $r = 16 \pm 2$.

A dramatic change in the turbulence regime of the solar wind takes place at heliocentric distances in the interval $8 < r < 20$. The spectral power index of electron density fluctuations is equal to 3.66 ± 0.1 at distances $r > 20$ (corresponding to the Kolmogorov spectrum), but decreases to 3 ± 0.2 at heliocentric distances $3 < r < 5$. The inner scale of density inhomogeneities is proportional to the heliocentric distance, increasing from 10 km at $r = 10$–32 km at $r = 25$. This order of magnitude corresponds to the proton gyroradius. Continuous registration of radiowave frequency fluctuations over a long period of time allows a determination of the outer scale of density inhomogeneities. This is also directly proportional to heliocentric distance, reaching a value of $1.5 \cdot 10^6$ km at the heliocentric distance $r = 10$.

Estimates of the amplitude of the fractional density fluctuations ($\gamma = \sigma_N/N$) derived from coronal radio-sounding observations are approximations, because the electron density (N) and its standard deviation (σ_N) were determined during different time periods. The amplitude of the fractional density fluctuation can vary from a minimum ~0.05 to a maximum ~0.25. The heliocentric distance dependence may depend upon whether the solar wind is in the fast or slow mode.

Acknowledgements

We are grateful to A.I. Efimov for helpful discussions. We appreciate the contributions of Prof. M.K. Bird and the other anonymous reviewer to the improvement of the text in its revised version.

References

Anderson, J.D., Krisher, T.P., Borutzki, S.E., et al., 1987. Radio range measurements of coronal electron densities during the solar conjunction of Voyager-2. Astrophys. J. 323 (2), 141–143.

Armand, N.A., Efimov, A.I., Yakovlev, O.I., 1987. A model of the solar wind turbulence from radio occultation experiments. Astron. Astrophys. 183, 135–141.

Armand, N.A., Efimov, A.I., Yakovlev, O.I., Yakubov, V.P., Vyshlov, A. S., Nabatov, A.S., Kaftonov, A.S., Rubtsov, S.N., Korsak, O.M., 1988. Frequency fluctuations of the decimeter and centimeter radio waves at the communication with spacecraft Venera-15,-16 through near-Sun plasma. Sov. J. Commun. Technol. Electron. 33, 54–60.

Armstrong, J.W., Woo, R., 1981. Solar wind motion within 30R, spacecraft radioscintillation observations. Astron. Astrophys. 103, 415–421.

Bird, M.K., 1982. Coronal investigations with occulted spacecraft signals. Space Sci. Rev. 33, 99–126.

Bird, M.K., Edenhofer, P., 1990. Remote sensing of the solar corona. In: Schwenn, R., Marsch, E. (Eds.), Physics of the Inner Heliosphere. Springer-Verlag, Heidelberg, pp. 13–97.

Bird, M.K., Volland, H., Paetzold, M., Edenhofer, P., Asmar, S.W., Brenkle, J.P., 1994. The coronal electron density distribution determined from dual – frequency ranging measurements during the 1991 solar conjunction of the Ulysses spacecraft. Astrophys. J. 426 (1), 373–381.

Bird, M.K., Paetzold, M., Edenhofer, P., Asmar, S.W., McElrath, T.P., 1996. Coronal radio sounding with Ulysses: solar wind electron density during the 1995 conjunction. Astron. Astrophys. 316, 441–448.

Chashei, I.V., Efimov, A.I., Samoznaev, L.N., Plettemeier, D., Bird, M. K., 2005. Properties of solar wind turbulence near the sun as deduced from coronal radio sounding. Adv. Space Res. 36 (8), 1454–1460.

Chashei, I.V., Efimov, A.I., Bird, M.K., 2007. Solar wind turbulence from radio occultation data. Astron. Astrophys. Trans. 26 (6), 611–620.

Efimov, A.I., Yakovlev, O.I., Razmanov, V.M., Shtrykov, V.K., 1977. Turbulence of plasma near the sun and the solar wind velocity derived from the Venera 10 radiooccultation experiment. Astron. Lett. 3 (7), 172–180.

Efimov, A.I., Yakovlev, O.I., Shtrykov, V.K., Rogalskii, V.I., Tukhonov, V.F., 1981. Spaced observations of frequency and phase fluctuations of radio waves scattering by the near-solar plasma. Radio Eng. Electron. 26 (2), 311–320.

Efimov, A.I., Yakovlev, O.I., Rubzov, S.N., 1987. Temporal specters of the amplitude fluctuations of the radio waves of centimeter and decimeter bands spacecraft Venera-15 and Venera-16 at radio sounding of the near Sun plasma. Sov. J. Commun. Technol. Electron. 32 (10), 1902–1914.

Efimov, A.I., Chashei, I.V., Shishov, V.I., Yakovlev, O.I., 1990. Solar wind acceleration: radio occultation data. Cosm. Res. 28 (4), 498–503.

Efimov, A.I., Samoznaev, L.N., Andreev, V.E., Bird, M.K., Edenhofer, P., Plettemeier, D., Wohlmuth, R., 2002a. East – west scattering level asymmetry of the solar corona. Adv. Space Res. 30 (3), 453–458.

Efimov, A.I., Chashei, I.V., Samoznaev, L.N., Andreev, V.E., Edenhofer, P., Plettemeier, D., Wohlmuth, R., 2002b. The outer scale of solar-wind turbulence from GALILEO coronal-sounding data. Astron. Rep. 46 (7), 579–590.

Efimov, A.I., Bird, M.K., Chashei, I.V., 2003. Simultaneous observations of radio wave frequency and intensity fluctuations for estimates of solar wind speed. Adv. Space Res. 32 (4), 485–490.

Efimov, A.I., Chashei, I.V., Bird, M.K., Plettemeier, D., Edenhofer, P., Wohlmuth, R., 2005a. Turbulence of the inner solar wind at solar maximum: coronal radio sounding with Galileo in 1999. Adv. Space Res. 36, 1448–1453.

Efimov, A.I., Bird, M.K., Rudas, V.K., Andreev, V.E., Chashei, I.V., Plettemeier, D., Edenhofer, P., 2005b. Solar wind velocity measurements near the sun using Ulysses radio amplitude correlation at two frequencies. Adv. Space Res. 35, 2189–2194.

Efimov, A.I., Armand, N.A., Lukanina, L.A., Samoznaev, L.N., Chashei, I.V., Bird, M.K., Plettemeier, D., 2008a. Radial dependence of the level of amplitude fluctuations of spacecraft signals probing circumsolar plasma. J. Commun. Technol. Electron. 53 (10), 1186–1194.

Efimov, A.I., Samoznaev, L.N., Bird, M.K., Chashei, I.V., Plettemeier, D., 2008b. Solar wind turbulence during the solar cycle deduced from Galileo coronal radio – sounding experiments. Adv. Space Res. 42 (2), 117–123.

Efimov, A.I., Lukanina, L.A., Samoznaev, L.N., Chashei, I.V., Bird, M. K., Plettemeier, D., 2009. Analysis of radio wave frequency fluctuations in the circumsolar plasma: Galileo coronal sounding data. J. Commun. Technol. Electron. 54 (7), 733–743.

Efimov, A.I., Lukanina, L.A., Samoznaev, L.N., Chashei, I.V., Bird, M.K., 2010a. Frequency fluctuation of spacecraft radio signals in the circumsolar plasma. J. Commun. Technol. Electron. 55 (11), 1253–1259.

Efimov, A.I., Imamura, T., Oyama, K., Noguchi, K., Samoznaev, L.N., Nabatov, A.S., Bird, M.K., Chashei, I.V., 2010b. Solar wind turbulence from radio-occultation experiments with the NOZOMI spacecraft. AstronomyReports 54 (11), 1032–1041.

Efimov, A.I., Lukanina, L.A., Samoznaev, L.N., Chashei, I.V., Bird, M. K., 2010c. Spatial distribution of turbulence characteristics in the inner solar wind. Astron. Rep. 87 (5), 446–455.

Efimov, A.I., Lukanina, L.A., Rudash, V.K., Samoznaev, L.N., Chashei, I. V., Bird, M.K., Paetzold, M., 2013. Frequency fluctuations of coherent signals from spacecraft observed during dual-frequency radio sounding of the circumsolar plasma in 2004–2008. Cosm. Res. 51 (1), 13–22.

Efimov, A.I., Lukanina, L.A., Samoznaev, L.N., Rudash, V.K., Chashei, I.V., Bird, M.K., Paetzold, M., 2014. Two – way frequency fluctuations observed during coronal radio sounding experiments. Sol. Phys. 289 (5), 1715–1729.

Efimov, A.I., Lukanina, L.A., Samoznaev, L.N., Chashei, I.V., Bird, M. K., Paetzold, M., 2017. Frequency fluctuations in the solar corona investigated with radio sounding experiments on the spacecraft ROSETTA and MARS EXPRESS in 2010/2011. Adv. Space Res. 59, 1652–1662.

Goldstein, R.M., 1969. Superior conjunction of Pioner 6. Science 166, 598.

Imamura, T., Tokumaru, M., Isobe, H., Shiota, D., Ando, H., Miyamoto, M., Toda, T., 2014. Outflow structure of the quiet sun corona probet by spacecraft radio scintillation in strong scattering. Astrophys. J. 788, 117–135.

Ishimaru, A., 1978. Wave Propagation and Scattering in Random Media, vol. 2. Academic Press, New York.

Janardhan, P., Bird, M., Edenhofer, P., Wohlmuth, R., Plettemeier, D., Asmar, S.W., Paetzold, M., 1999. Coronal velocity measurements with Ulysses: multi-link correlation studies during two superior conjunctions. Solar Phys. 184 (1), 157–172.

Jensen, E.A., Frazin, R., Heiles, C., 2016. The comparison of total electron content between radio and Thompson scattering. Solar Phys. 291, 465–471.

Kolosov, M.A., Yakovlev, O.I., Efimov, A.I., 1978. Investigation of the propagation of the decimeter radio waves at the flight of the interplanetary station Venere-10. Radio Eng. Electron. Phys. 23 (9), 1729–1738.

Kolosov, M.A., Yakovlev, O.I., Efimov, A.I., et al., 1982. Decimeter radio wave propagation in the turbulent plasma near the sun, using Venera10 spacecraft. Radio Sci. 17 (3), 664–674.

Krisher, T.P., Anderson, J.D., Morabito, D.D., et al., 1991. Radio range measurements of coronal electron densities at 13 and 3.6 centimeter wavelengths during 1988 solar conjunction. Astrophys. J. Part2 – Lett. 375 (1), L57–L60.

Muhleman, D.O., Esposito, P.B., Anderson, J.D., 1977. The electron density profile of the outer corona and the interplanetary medium from Mariner-6 and Mariner-7 time delay measurements. Astrophys. J. 211 (3), 943–957.

Muhleman, D.O., Anderson, J.D., 1981. Solar wind electron densities from Viking dual – frequency radio measurements. Astrophys. J. 247 (3), 1093–1101.

Paetzold, M., Bird, M.K., Edenhofer, P., et al., 1995. Dual – frequency radio sounding of the solar corona during the 1995 conjunction of the Ulysses spacecraft. Geophys. Res. Lett. 22 (23), 3313–3317. https://doi.org/10.1029/95GL03184.

Paetzold, M., Bird, M.K., 1998. Polar plumes and fine – scale coronal structures of radio sounding data. Geophys. Res. Lett. 25, 1845–1849.

Paetzold, M., Hahn, M., Tellmann, S., Hausler, S., Bird, M.K., Tyler, G. L., Asmar, S.W., Tsurutani, B.T., 2012. Coronal density structures and CMEs: superior solar conjunctions of Mars Express, Venus Express, and Rosetta: 2004, 2006, and 2008. Solar Phys. 279, 127–152.

Pisanko Yu. V., 1996. The global solar magnetic field as a "controller" for the origin and acceleration model of solar wind streams. Adv. Space Res. 17(3), (3)61–(3)64.

Ramzanov, V.M., Efimov, A.I., Yakovlev, O.I., 1979. Formation of spectral lines of radio signal propagation in near-solar plasma. Radiophys. Quantum Electron. 22 (9), 729–734.

Rubzov, S.N., Yakovlev, O.I., Efimov, A.I., 1987. Density irregularity and kinetic energy of the solar wind according to the coronal sounding experiments with spacecraft Venera-15 and Venera-16. Cosm. Res. 25 (4), 520–527.

Tyler, G.L., Vesecky, J.F., Plume, M.A., et al., 1981. Radio wave scattering observations of the solar corona First-order measurements of expansion velocity and turbulence spectrum using Viking and Mariner-10 spacecraft. Astrophys. J. 249, 318–332.

Weisberg, J.M., Rankin, J.M., Payne, R.R., Counselman III, C.C., 1976. Further changes in the distribution of density and radio scattering in the solar corona in 1973. Ap. J. 209, 252–258.

Wohlmuth, R., Plettemeier, D., Edenhofer, P., et al., 1997. Measurement of the propagation speed of plasma inhomogeneities in the solar corona using an uplink/downlink cross – correlation method. Radio Sci. 32 (2), 617–628.

Woo, R., Yang, F.C., Ishimaru, A., 1976a. Structure of density fluctuations near the sun deduced from Pioner-6 spectral broadening measurements. Astrophys. J. 210, 593–602.

Woo, R., Yang, F.C., Yip, K., Kendall, W.B., 1976b. Measurements of large-scale density fluctuations in the solar wind using dual-frequency phase scintillations. Astrophys. J. 210, 568–574.

Woo, R., 1978. Radial dependence of solar wind properties deduced from Helios-1,2 and Pioneer-10,11 radio scattering observations. Astrophys. J. 219, 727–739.

Woo, R., Armstrong, J.W., Bird, M.K., Paetzold, M., 1995. Variation of fractional electron density fluctuations using 40R observed by Ulysses ranging measurements. Geophys. Res. Lett. 22 (4), 329–332.

Woo, R., 1996. 1985 Voyager-2 radio ranging measurements of coronal density. Astrophys. J. 458, 87–93.

Yakovlev, O.I., Trusov, B.P., Efimov, A.I., et al., 1974. A study of decimeter radio-wave propagation in solar plasma environment by means of "Mars-2" spacecraft. Cosm. Res. 12 (4), 600 (in Russian).

Yakovlev, O.I., Molotov, E.P., Kruglov, Y.M., Efimov, A.I., Razmanov, V.M., 1977. Peculiarities of propagation of radio waves through the solar plasma, based on data supplied by Mars-2 and Mars-7 transmitters. Radio Eng. Electron. Phys. 22 (2), 29–35.

Yakovlev, O.I., Efimov, A.I., Razmanov, V.M., Shtrykov, V.K., 1980a. Irregular structure and velocity of near sun plasma from the data of "Venera 10" spacecraft. Astron. Rep. 57 (4), 790–796.

Yakovlev, O.I., Efimov, A.I., Razmanov, V.M., Shtrykov, V.K., 1980b. Radio wave propagation in the turbulent solar plasma using three satellites. Acta Astronaut. 7, 235–242.

Yalovlev, O.I., Efimov, A.I., Rubzov, S.N., 1987. Dynamics and turbulence of the solar wind in the forming region according to the radio occultation experiments with the spacecraft Venera-15 and Venera-16. Cosm. Res. 25 (2), 208–217.

Yakovlev, O.I., Efimov, A.I., Molotov, E.P., 1988a. Amplitude fluctuations of decimeter and centimeter radio waves emitted by the Venera-15 and Venera-16 space probes during propagation through the solar plasma. Radiophys. Quantum Electron. 31 (1), 1–6.

Yakovlev, O.I., Efimov, A.I., Rubtsov, S.N., 1988b. Solar wind from radiooccultation data using Venera 15 and Venera 16 spacecraft. Astron. Rep. 32 (6), 672–677.

Yakovlev, O.I., Efimov, A.I., Yakubov, V.P., 1989. Occultation of the plasma near sun and the speed of the solar wind: fluctuations in the frequency and phase of radio waves at two separated points by Venera-15 and Venera-16 space probes. Radiophys. Quantum Electron. 32 (5), 391–396 (in Russian).

Yakovlev, O.I., 2002. Space Radio Science. Taylor - Francis, p. 307.

Yakubov, V.P., Yakovlev, O.I., Efimov, A.I., Erofeev, A.P., 1991. The solar wind velocity as determined from two-way Doppler measurements for near-sun radio sounding. Radiophys. Quantum Electron. 34 (6), 615–623.